PERGAMON

International Journal of Solids and Structures 38 (2001) 8207–8218

INTERNATIONAL JOURNAL OF SOLIDS and STRUCTURES

www.elsevier.com/locate/ijsolstr

Wave propagation in a piezoelectric coupled cylindrical membrane shell

Q. Wang *

Department of Civil Engineering, National University of Singapore, 10 Kent Ridge Crescent, Singapore 119260, Singapore

Received 22 December 2000; in revised form 21 February 2001

Abstract

Wave propagation in a piezoelectric coupled cylindrical shell structure is investigated in the paper. The membrane shell model is used, hence, the transverse forces, bending and twisting moments are considered negligible in this thin cylindrical shell structure. The decoupled torsional wave velocity and the dispersive curves for the two-mode shell model are obtained theoretically. The cut-off frequency and phase velocities at limit cases of wave number are also derived. The mechanical coupling effect by the piezoelectric layer in the torsional phase is clearly observed. The piezoelectric effect by the piezoelectric layer in the two-mode phase velocities obtained from coupled equations and the cut-off frequency of the structure is studied by changing the thickness of the piezoelectric layer. The results of this paper can serve as a reference for future study on wave propagation in coupled structures as well as in the design of smart structures incorporating piezoelectric materials.

Keywords: Dispersive curves; Piezoelectric coupled shell; Membrane shells; Cut-off frequency; Torsional phase velocity

1. Introduction

The membrane shell model was put forth by Love (1944), in which the transverse forces, bending and twisting moments are negligible. Such model is suitable for thin shell structures in which only normal and shear forces acting in the mid-surface of the shell are considered. Although it is a low-order shell model, it is easy to present the essential features of the shell, and what is more, it provides basic model for higher-order shell model in which shear and twisting effects are considered. Some slight modified theories based on this simply model was presented by Flügger (1934), Vlasov (1949), Donnel (1933), Sanders (1959). Mirsky and Herrmann (1958) included shear effects in both the axial and circumferential direction and rotary-inertia effects in the study of axially symmetric waves in a cylindrical shell. Lin and Morgan (1956) developed the equations for axially symmetric motions including shear effects and rotary-inertia effects. Cooper and

* Tel.: +65-874-4683; fax: +65-779-1635.
E-mail address: cvewangq@nus.edu.sg (Q. Wang).

0020-7683/01/$ - see front matter
PII: S0020-7683(01)00071-3

Naghdi (1957) presented a theory including shear effects and rotary inertia for non-axially symmetric motion of shell structures.

The researches and applications on smart materials and structures, especially the uses of piezoelectric materials, have recently been studied widely. To provide accurate mechanics model is the key to the studies of the piezoelectric materials. Basic mechanics models for the interaction of structures coupled with piezoelectric actuators and sensors, either surface bonded on or embedded in the host beam structure, have been proposed by several researchers (Bailey and Hubbards, 1985; Varadan et al., 1987; Crawley and de Luis, 1987; Wang and Rogers, 1991). The researches on wave propagation and vibration in pure piezoelectric structures have been received considerable attention previously as exhibited by the work of Mindlin (1952), Tiersten (1963) and Bleustein (1969). Research on its application for time delay devices has been conducted (Viktorov, 1967, 1981; Curtis and Redwood, 1973; Sun and Cheng, 1974). Studies on wave propagation in piezoelectric coupled structures are essential for the application of piezoelectric materials, such as the design of ultrasonic piezoelectric motor. Wave propagations in beam and plate structures based on the classical models and the refined models have been studied by Wang and Quek (Wang and Quek, 2001; Quek and Wang, 2001).

The objective of this paper is to present the results of axial symmetric wave motions in piezoelectric coupled membrane cylindrical shells by the basic membrane shell model. The dispersion curves for different ratios of the thickness of the piezoelectric layer to the thickness of the host shell structure, as well as different core materials of the cylindrical shell are obtained by the model. In addition, the phase velocity and cut-off frequency for limit wave number based on the model are also presented.

2. Governing equation for the piezoelectric coupled membrane shell

A thin shell surface bonded by a piezoelectric layer is shown in Fig. 1(a). Based on the membrane shell theory, only normal and shear forces acting at the mid-surface of the shell are considered. The transverse shear forces and the bending and twisting moments are assumed negligible small in this model. The coordinate is set to indicate the coordinates x for the direction along the shell, θ for the direction of polar angel, and r for the radial direction. The stress analysis on an infinitesimal element of the shell structure is shown in Fig. 1(b). The governing equations of motion in the longitudinal, tangential, and radial directions are, respectively (Graff, 1991),

$$\frac{\partial N_x}{\partial x}+\frac{\partial N_{\theta x}}{R\,\partial\theta}=(\rho h+\rho' h_1)\frac{\partial^2 u}{\partial t^2} \tag{1}$$

$$\frac{\partial N_\theta}{R\,\partial\theta}+\frac{\partial N_{x\theta}}{\partial x}=(\rho h+\rho' h_1)\frac{\partial^2 v}{\partial t^2} \tag{2}$$

$$-\frac{N_\theta}{R}=(\rho h+\rho' h_1)\frac{\partial^2 w}{\partial t^2} \tag{3}$$

where u, v, and w are the longitudinal, transverse, and radial displacement of the section; R is the radius of the shell; h and h_1 are thickness of the shell and layer; and ρ and ρ' are mass densities of the shell and the layer; N_x, $N_{\theta x}$, $N_{x\theta}$, and N_θ are membrane stresses shown in Fig. 1(b).

These membrane stresses are obtained by integrating the stresses across the thickness of the shell as follows:

$$N_x=\int_{-h/2}^{h/2}\sigma_x^1\,\mathrm{d}z+\int_{h/2}^{(h/2)+h_1}\sigma_x^2\,\mathrm{d}z \tag{4a}$$

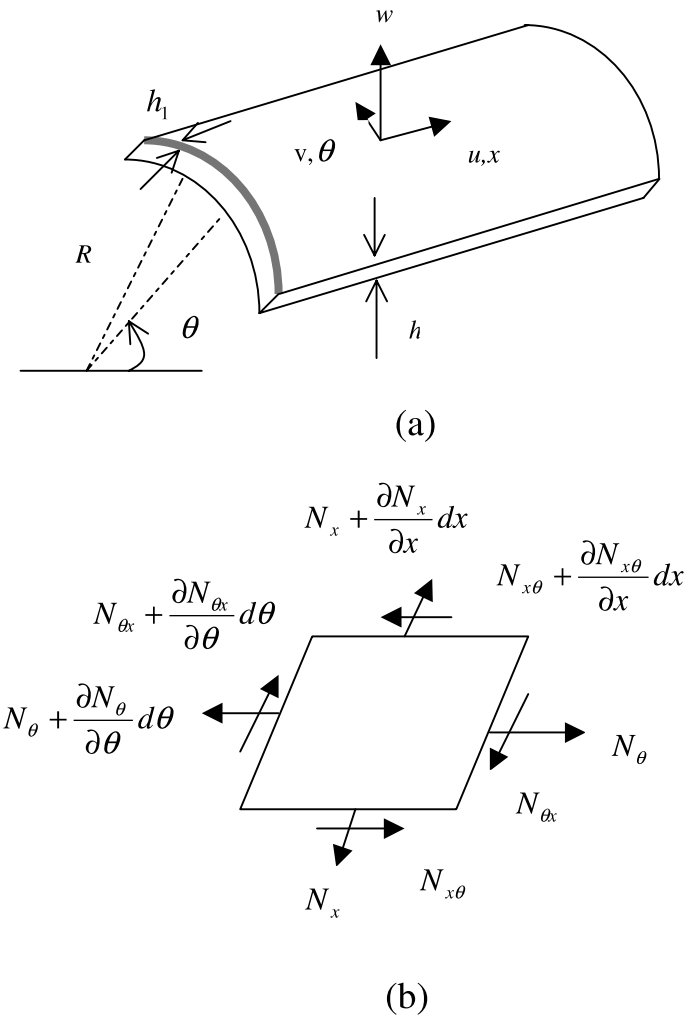

Fig. 1. A piezoelectric thin membrane shell (a) layout (b) the stress analysis at an infinitesimal element.

$$N_\theta = \int_{-h/2}^{h/2} \sigma_\theta^1 \, \mathrm{d}z + \int_{h/2}^{(h/2)+h_1} \sigma_\theta^2 \, \mathrm{d}z \tag{4b}$$

$$N_{\theta x} = N_{x\theta} = \int_{-h/2}^{h/2} \tau_{x\theta}^1 \, \mathrm{d}z + \int_{h/2}^{(h/2)+h_1} \tau_{x\theta}^2 \, \mathrm{d}z \tag{4c}$$

where σ_x, σ_θ, and $\tau_{x\theta}$ are the normal and shear stresses distributed in the host shell and the piezoelectric layer, and the superscripts 1 and 2 represent the variables in the host shell and the piezoelectric layer respectively.

The poling direction of the piezoelectric material is assumed to be in the axial x direction of shell, which also means the x direction is the axis of symmetry for the piezoelectric layer. The relationship of the strains ε_x, ε_θ, and $\gamma_{x\theta}$, and stresses σ_x, σ_θ, and $\tau_{x\theta}$ in the shell and piezoelectric layer may be obtained accordingly as

$$\sigma_x^1 = \frac{E}{1-\upsilon^2}(\varepsilon_x + \upsilon\varepsilon_\theta) \tag{5a}$$

$$\sigma_\theta^1 = \frac{E}{1-\upsilon^2}(\varepsilon_\theta + \upsilon\varepsilon_x) \tag{5b}$$

$$\tau_{x\theta}^1 = \gamma_{x\theta}\frac{E}{2(1+\upsilon)} \tag{5c}$$

$$\sigma_x^2 = c_{33p}\varepsilon_x + c_{13p}\varepsilon_\theta - e_{33p}E_x = c_{33p}\varepsilon_x + c_{13p}\varepsilon_\theta + e_{33p}\frac{\partial\varphi}{\partial x} \tag{6a}$$

$$\sigma_\theta^2 = c_{11p}\varepsilon_\theta + c_{13p}\varepsilon_x - e_{31p}E_x = c_{33p}\varepsilon_x + c_{13p}\varepsilon_\theta + e_{31p}\frac{\partial\varphi}{\partial x} \tag{6b}$$

$$\tau_{x\theta}^2 = c_{44p}\gamma_{x\theta} - e_{15p}E_\theta = c_{44p}\gamma_{x\theta} + e_{15p}\frac{\partial\varphi}{R\,\partial\theta} \tag{6c}$$

where φ is the variable of electric potential distributed in the piezoelectric layer; E and υ are the Young modulus and Poisson ratio of host shell material; $c_{33p} = c_{33} - (c_{13}^2/c_{11})$, $c_{13p} = c_{13} - (c_{12}c_{13}/c_{11})$, $c_{11p} = c_{11} - (c_{12}^2/c_{11})$, $c_{44p} = c_{44}$ are effective elastic module of the piezoelectric layer for plane stress problem; $e_{31p} = e_{31} - (c_{12}/c_{11})e_{31}$, $e_{15p} = e_{15}$, $e_{33p} = e_{33} - (c_{13}/c_{11})e_{31}$ are effective piezoelectric constants of the piezoelectric layer for plane stress problem.

The kinematics of the deformation of the shell is considered below. Under the membrane shell model, the corresponding strains in the current coordinate system are expressed as (Love, 1944)

$$\varepsilon_x = \frac{\partial u}{\partial x} \tag{7}$$

$$\varepsilon_\theta = \frac{1}{R}\left(w + \frac{\partial v}{\partial\theta}\right) \tag{8}$$

$$\gamma_{x\theta} = \frac{\partial v}{\partial x} + \frac{\partial u}{R\,\partial\theta} \tag{9}$$

Substituting Eqs. (7)–(9) into Eqs. (4a)–(4c) gives

$$N_x = A_1\frac{\partial u}{\partial x} + A_2\left(w + \frac{\partial v}{\partial\theta}\right) + A_4\frac{\partial\varphi}{\partial x} \tag{10}$$

$$N_{x\theta} = A_3\left(\frac{\partial v}{\partial x} + \frac{\partial u}{R\,\partial\theta}\right) + A_5\frac{\partial\varphi}{R\,\partial\theta} \tag{11}$$

$$N_\theta = B_1\left(w + \frac{\partial v}{\partial\theta}\right) + B_2\frac{\partial u}{\partial x} + A_6\frac{\partial\varphi}{\partial x} \tag{12}$$

where

$$A_1 = \frac{Eh}{1-\upsilon^2} + c_{33p}h_1, \quad A_2 = \frac{Eh\upsilon}{1-\upsilon^2} + c_{13p}h_1, \quad A_3 = \frac{Eh}{2(1+\upsilon)} + c_{44p}h_1, \quad A_4 = e_{33p}h_1,$$

$$A_5 = e_{15p}h_1, \quad A_6 = e_{31p}h_1, \quad B_1 = \frac{Eh}{1-\upsilon^2} + c_{11p}h_1, \text{ and } B_2 = \frac{Eh\upsilon}{1-\upsilon^2} + c_{13p}h_1.$$

Then Eqs. (1)–(3) become

$$A_1\frac{\partial^2 u}{\partial x^2}+A_2\left(\frac{\partial w}{\partial x}+\frac{\partial^2 v}{\partial x\,\partial\theta}\right)+A_3\left(\frac{\partial^2 v}{R\,\partial x\,\partial\theta}+\frac{\partial^2 u}{R^2\,\partial\theta^2}\right)+A_4\frac{\partial^2\varphi}{\partial x^2}+A_5\frac{\partial^2\varphi}{R^2\,\partial\theta^2}=\left(\rho h+\rho' h_1\right)\frac{\partial^2 u}{\partial t^2} \tag{13}$$

$$\frac{B_1}{R}\left(\frac{\partial w}{\partial\theta}+\frac{\partial^2 v}{\partial\theta^2}\right)+\frac{B_2}{R}\frac{\partial^2 u}{\partial x\,\partial\theta}+A_3\left(\frac{\partial^2 v}{\partial x^2}+\frac{\partial^2 u}{R\,\partial x\,\partial\theta}\right)+(A_5+A_6)\frac{\partial^2\varphi}{R\,\partial x\,\partial\theta}=\left(\rho h+\rho' h_1\right)\frac{\partial^2 v}{\partial t^2} \tag{14}$$

$$-\frac{B_1}{R}\left(w+\frac{\partial v}{\partial\theta}\right)-\frac{B_2}{R}\frac{\partial u}{\partial x}-A_6\frac{\partial\varphi}{R\,\partial x}=\left(\rho h+\rho' h_1\right)\frac{\partial^2 w}{\partial t^2} \tag{15}$$

The variables for electric displacements in the piezoelectric layer, on the other hand, are expressed as follows:

$$D_x=-\Xi_{33p}\frac{\partial\varphi}{\partial x}+e_{33p}\varepsilon_x+e_{31p}\varepsilon_\theta \tag{16}$$

$$D_\theta=-\Xi_{11p}\frac{\partial\varphi}{R\,\partial\theta}+e_{15}\gamma_{x\theta} \tag{17}$$

$$D_r=0 \tag{18}$$

where $\Xi_{33p}=\Xi_{33}+(e_{31}^2/c_{11})$, $\Xi_{11p}=\Xi_{11}+(e_{15}^2/c_{55})$, are effective dielectric coefficients in the piezoelectric layer for plane stress problem.

Satisfying the Maxwell equation $\nabla D=0$, in view of Eqs. (16)–(18), yields

$$-\Xi_{33p}\frac{\partial^2\varphi}{\partial x^2}-\Xi_{11p}\frac{\partial^2\varphi}{R^2\,\partial\theta^2}+e_{33p}\frac{\partial^2 u}{\partial x^2}+\frac{e_{13p}}{R}\left(\frac{\partial w}{\partial x}+\frac{\partial^2 v}{\partial x\,\partial\theta}\right)+e_{15}\left(\frac{\partial^2 v}{\partial x\,\partial\theta}+\frac{\partial^2 u}{R\,\partial\theta^2}\right)=0 \tag{19}$$

3. Dispersive characteristics

The most important special case results from the axisymmetric motion. Thus, if $\partial/\partial\theta=0$, Eqs. (13)–(15) and (19) become

$$A_1\frac{\partial^2 u}{\partial x^2}+A_2\frac{\partial w}{\partial x}+A_4\frac{\partial^2\varphi}{\partial x^2}=(\rho h+\rho' h_1)\frac{\partial^2 u}{\partial t^2} \tag{20}$$

$$A_3\frac{\partial^2 v}{\partial x^2}=(\rho h+\rho' h_1)\frac{\partial^2 v}{\partial t^2} \tag{21}$$

$$-\frac{B_1}{R}w-\frac{B_2}{R}\frac{\partial u}{\partial x}-A_6\frac{\partial\varphi}{R\partial x}=(\rho h+\rho' h_1)\frac{\partial^2 w}{\partial t^2} \tag{22}$$

$$-\Xi_{33p}\frac{\partial^2\varphi}{\partial x^2}+e_{33p}\frac{\partial^2 u}{\partial x^2}+\frac{e_{13p}}{R}\frac{\partial w}{\partial x}=0 \tag{23}$$

For the general case of wave propagation in the piezoelectric coupled shell structure, the cross-section of the shell can be very complicated. It is better to use higher-order shell model and include the transverse effects in the model which are beyond the scope of the current paper.

It can be observed that Eq. (21) is decoupled from the remaining equations, which can be written as

$$\frac{\partial^2 v}{\partial x^2} = \frac{1}{c_t^2}\frac{\partial^2 v}{\partial t^2} \tag{24}$$

where $c_t = \sqrt{\frac{A_3}{\rho h + \rho' h_1}} = \sqrt{\frac{Gh + c_{44} h_1}{\rho h + \rho' h_1}}$, and $G = \frac{E}{2(1+\upsilon)}$.

As indicated by Love (1944), this is the pure torsional motion of the shell. It can be seen clearly from the expression of the phase velocity in the above that the piezoelectric layer plays a role as a composite part in the structure, as the elastic modulus c_{44p} is shown in the expression. Its mechanical coupling effect is quite obvious. However, no piezoelectric effect is found in the case, for no piezoelectric coefficients or dielectric constants are involved in the expression of the torsional phase velocity.

Now consider the wave propagation from the other governing equations by letting,

$$u = U e^{i\xi(x-ct)} \tag{25a}$$

$$w = W e^{i\xi(x-ct)} \tag{25b}$$

$$\varphi = \Phi e^{i\xi(x-ct)} \tag{25c}$$

where ξ and c are wave number and wave phase velocity respectively; U, W, and Φ are magnitudes of variables of the wave propagation.

Substituting wave solutions into Eq. (23) yields

$$\Phi = \frac{e_{33p}}{\Xi_{33p}} U - \frac{i e_{13p}}{R \Xi_{33p} \xi} W \tag{26}$$

Then Eq. (26) will result in the relationship between variables U and W from Eq. (22) as

$$W = i\xi L_1 U \tag{27}$$

where

$$L_1 = \frac{D_1}{(\rho h + \rho' h_1)\omega^2 - D_2}, \quad D_1 = \frac{1}{R}\left(B_2 + \frac{A_6 e_{33p}}{\Xi_{33p}}\right), \quad D_2 = \frac{1}{R}\left(B_1 + \frac{A_6 e_{31p}}{\Xi_{33p}}\right).$$

Introducing Eq. (27) into Eq. (26) gives

$$\Phi = L_2 U \tag{28}$$

where

$$L_2 = D_3 + D_4 L_1, \quad D_3 = \frac{e_{33p}}{\Xi_{33p}}, \quad D_4 = \frac{e_{31p}}{R \Xi_{33p}}.$$

Substituting Eqs. (26) and (27) into Eq. (20), we have

$$(-A_1 \xi^2 - \frac{A_2}{R} L_1 \xi^2 - A_4 L_2 \xi^2) U = -(\rho h + \rho' h_1)\omega^2 U \tag{29}$$

The dispersive solution for this piezoelectric coupled membrane shell is then obtained as

$$(\rho h + \rho' h_1)c^2 - A_1 - \frac{A_2}{R} L_1 - A_4 L_2 = 0 \tag{30}$$

The solutions for c^2 in Eq. (30) are expressed as:

$$c_1 = \left(\frac{1}{2}\left(-E_2 - \sqrt{E_2^2 - 4E_1 E_2}\right)\right)^{1/2} \tag{31a}$$

$$c_2 = \left(\frac{1}{2}\left(-E_2 + \sqrt{E_2^2 - 4E_1E_2}\right)\right)^{1/2} \tag{31b}$$

where

$$E_1 = (\rho h + \rho' h_1)^2\xi^2, \quad E_2 = -D_2(\rho h + \rho' h_1) - A_1(\rho h + \rho' h_1)\xi^2 - A_4D_3(\rho h + \rho' h_1)\xi^2,$$
$$E_3 = A_1D_2 - A_2D_1 + A_4(D_3D_2 - D_4D_1).$$

Consider the large and small wavelength limits. As $\xi \to 0$, the cut-off frequencies are

$$\omega_1 = 0, \quad \text{and} \quad \omega_2 = \frac{1}{R}\sqrt{\left(\frac{Eh}{1-\upsilon^2} + c_{11p}h + \frac{e_{13p}^2 h}{\Xi_{33p}}\right)\Big/(\rho h + \rho' h_1)} \tag{32}$$

If no piezoelectric layer is bonded on the shell, i.e. $h_1 = 0$, we have

$$\omega_2 = \frac{1}{R}\sqrt{\frac{E}{\rho(1-\upsilon^2)}} \tag{33}$$

The corresponding phase velocity is

$$c^2 = \frac{1}{D_2(\rho h + \rho' h_1)}(A_4D_3D_2 - A_4D_4D_1 + A_1D_2 - \frac{A_2}{R}D_1) \tag{34}$$

and we have the velocity at limit case, $h_1 = 0$,

$$c^2 = \frac{E}{\rho} \tag{35}$$

As $\xi \to \infty$, the results are

$$c^2 = \frac{1}{\rho h + \rho' h_1}(A_1 + A_4D_3) \tag{36}$$

and

$$c^2 = \frac{E}{\rho(1-\upsilon^2)} \tag{37}$$

when there is no piezoelectric layer in the model, i.e. $h_1 = 0$.

Those results at $h_1 = 0$ shown above are consistent with the results for pure metal cylindrical shell (Love, 1944).

4. Numerical simulations

In Table 1, the material properties of the host shell of aluminium, steel, and gold, and the piezoelectric layer of PZT4 are listed for numerical analysis. To investigate the effect by the piezoelectric layer in Figs. 2–5, the non-dimensional torsional velocity $\bar{c}_t$, first mode phase velocity $\bar{c}_1$, second mode phase velocity $\bar{c}_2$, and the cut-off frequency $\bar{\omega}$ are defined below:

$$\bar{c}_t = c_t \Big/ \sqrt{\frac{E}{2\rho(1+\upsilon)}} \tag{38}$$

$$\bar{c}_1 = c_1 \Big/ \sqrt{\frac{E}{\rho}} \tag{39}$$

Table 1
Material properties

	Aluminium	Steel	Gold	PZT-4
Mass density (kg/m^3)	$\rho' = 2.8 \times 10^3$	$\rho' = 7.8 \times 10^3$	$\rho' = 1.9 \times 10^4$	$\rho = 7.5 \times 10^3$
Young modulus (N/m^2)	$E = 70 \times 10^9$	$E = 200 \times 10^9$	$E = 78 \times 10^{10}$	$c_{11} = 132 \times 10^9$ $c_{33} = 115 \times 10^9$ $c_{12} = 71 \times 10^9$
Poisson ratio	0.33	0.28	0.42	$c_{13} = 73 \times 10^9$ $c_{44} = 26 \times 10^9$
e_{31} (k/m^2)				-4.1
e_{33} (k/m^2)				14.1
e_{15} (k/m^2)	–	–	–	10.5
Ξ_{11} (ϕ/m)	–	–	–	5.841×10^{-9}
Ξ_{33} (ϕ/m)	–	–	–	7.124×10^{-9}

$$\bar{c}_2 = c_2 \Big/ \sqrt{\frac{E}{\rho(1-\upsilon^2)}} \tag{40}$$

$$\bar{\omega} = R\omega \Big/ \sqrt{\frac{E}{\rho(1-\upsilon^2)}} \tag{41}$$

First, the torsional phase velocities of the membrane shell with core materials of aluminium, steel, and gold surface bonded by PZT-4 are plotted in Fig. 2 as a function of thickness of the piezoelectric layer. As indicated in the paper, this sort of phase velocity is obtained from a decoupled equation, and the piezoelectric layer plays a role as a "composite" part, which means that only its mechanical effect are modelled in the torsional phase velocity of this piezoelectric coupled structure, whereas, its piezoelectric effects are not involved. Since the torsional stiffness of PZT is smaller than that of aluminium and steel, but greater than that of gold. It is natural to see from Fig. 2 that the phase velocity increase as the thickness of the

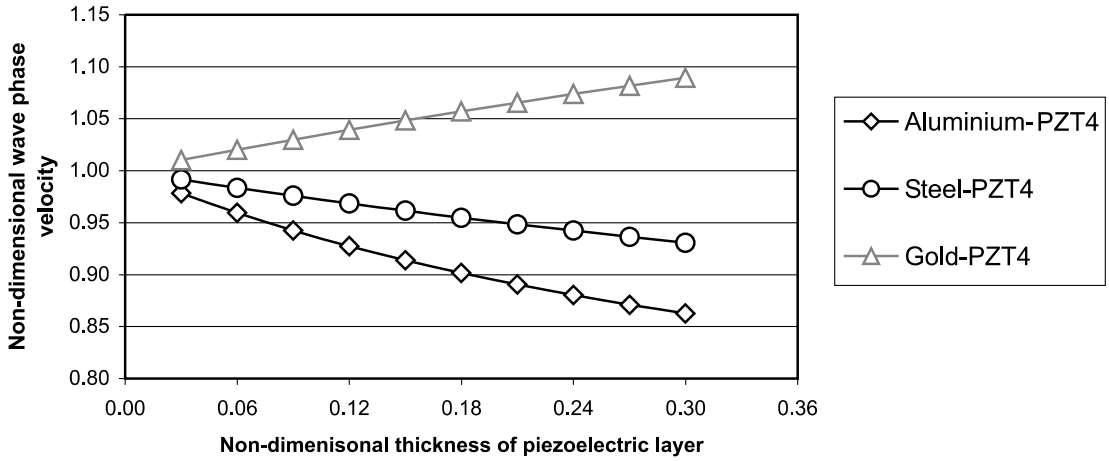

Fig. 2. Torsional wave phase velocity of the shell structure versus the thickness of piezoelectric layer.

piezoelectric layer increases for the shell with gold as core material. The inverse trend is found in the case of steel and aluminium as core materials, in which thicker layers correspond to lower phase velocities.

The limit cases for first mode velocity as wave number goes to zero and second mode velocity as wave number goes to infinite and cut-off frequency are also studied in Figs. 3–5. From Eqs. (34), (36), and (33), it is observed the effects by the piezoelectric layer not only lie in its mechanical coupling effect but also relate to its piezoelectric coupling effect as shown in the equations that its piezoelectric coefficients and dielectric constants are all involved. Similar results are found in Figs. 3–5 that for the core of aluminium and steel, the variables under investigation all decrease as the piezoelectric layer becomes thicker. However, for the shell with gold as core material, the first and second mode phase velocities and the cut-off frequency increase as the piezoelectric layer increases.

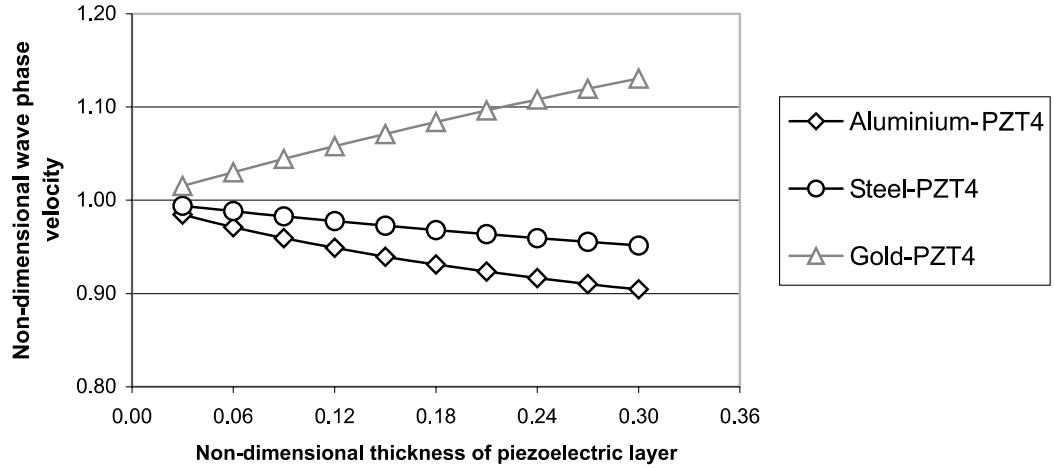

Fig. 3. First mode phase velocity of the shell structure at zero wave number versus the thickness of piezoelectric layer.

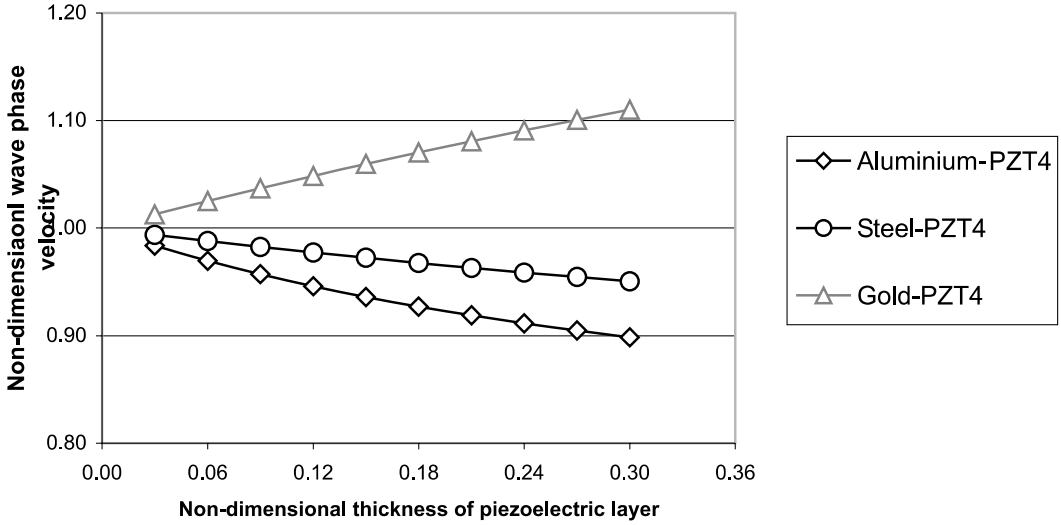

Fig. 4. Second mode phase velocity of the shell structure at infinite wave number versus the thickness of piezoelectric layer.

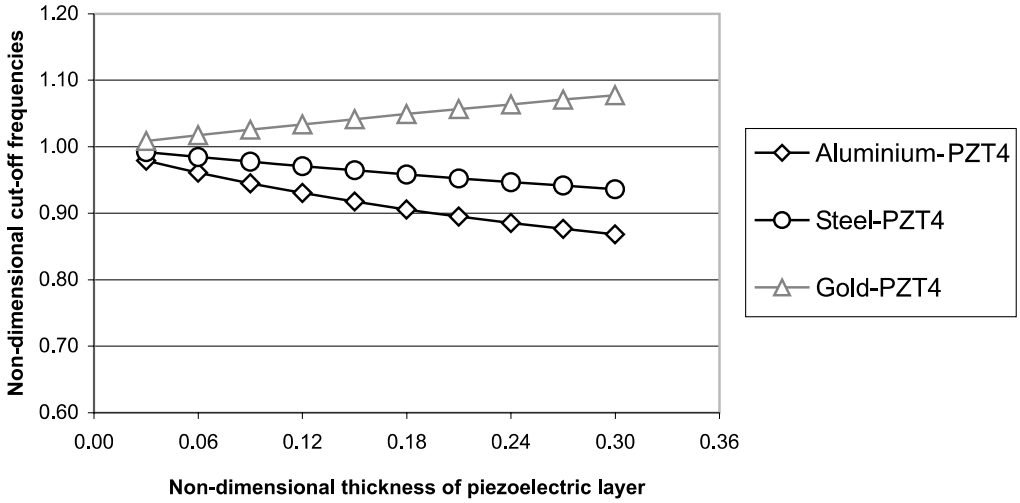

Fig. 5. Cut-off frequencies versus the thickness of piezoelectric layer.

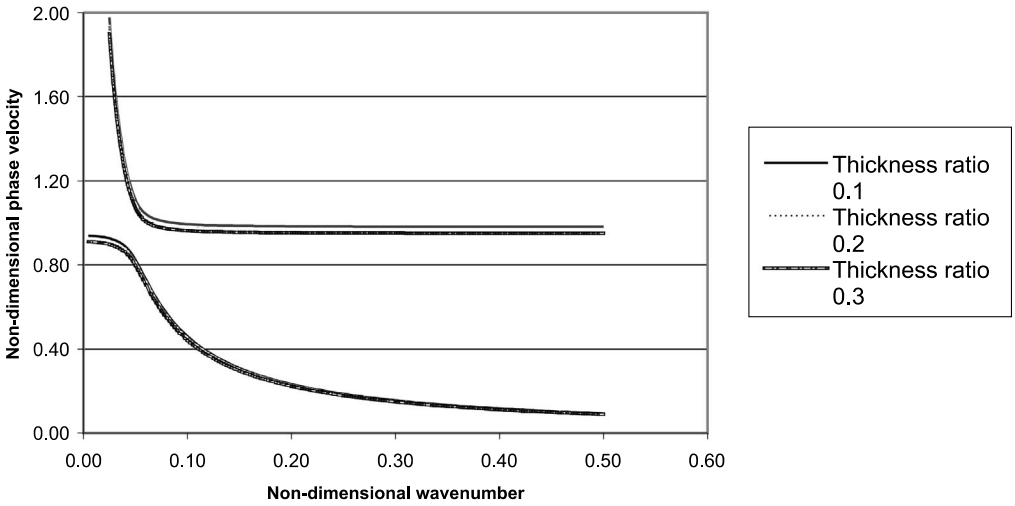

Fig. 6. Dispersive curves of steel–PZT-4 shell structure.

In Figs. 6 and 7, the dispersive curves for the first and second mode phase velocities are plotted for the piezoelectric coupled shell structures with steel and gold as core materials respectively. The non-dimensional phase velocities are defined as $v = v/\sqrt{E/\rho(1-v^2)}$ in these two figures. The phase velocity for the first mode at small wave number approaches to the phase velocity in Eq. (34) which is obtained in the limit case of zero wave number. The phase velocity for the second mode approaches to infinite in this case as seen in Figs. 6 and 7 which coincides with the solution for a pure metal shell (Graff, 1991). At infinite wave number, the phase velocity for the second mode approaches to the value obtained in Eq. (36) which is obtained in the limit case of infinite wave number, i.e. small wavelength. Different ratios of the thickness of the piezoelectric layer to the thickness of the host shell are also plotted in these figures. An interesting phenomenon is that the first mode phase velocity converges for different thickness of the piezoelectric layer.

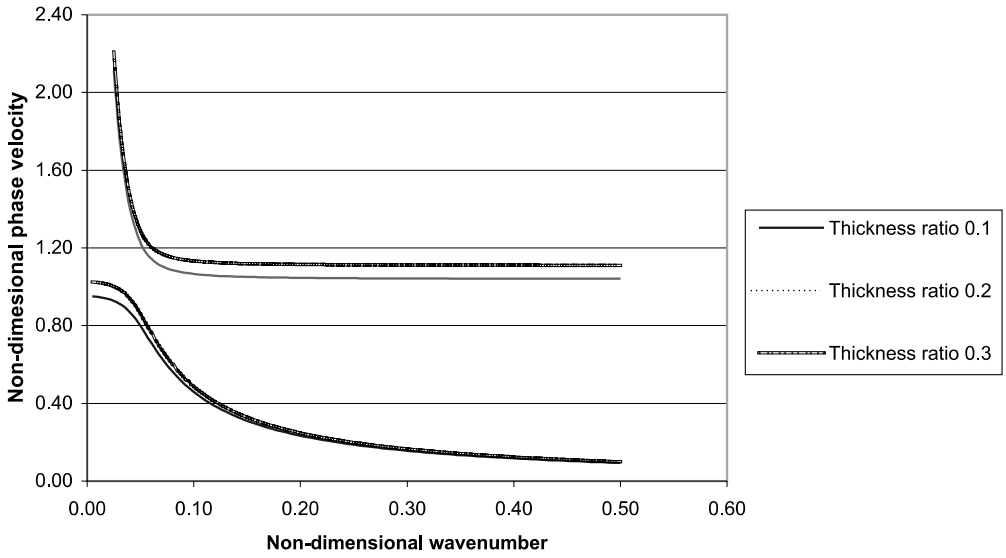

Fig. 7. Dispersive curves of gold–PZT-4 shell structure.

5. Concluding remarks

In this paper, the wave propagation in a piezoelectric coupled cylindrical membrane shell is presented. The transverse forces, bending and twisting moments are assumed negligible in the membrane shell model. The axisymmetric motion is then investigated in the paper, and the general motion of wave propagation in the shell structure is left for further studies by higher-order shell models.

The torsional phase velocity is first derived by solving a decoupled equation of the shell structure. From the theoretical analysis, it shows that the piezoelectric coefficients and dielectric constants are not appeared in the expression of the velocities, and thus no piezoelectric effects are found in the torsional phase velocity. On the other hand, the piezoelectric effects are clearly indicated from the derivation of the first mode and second mode phase velocities and cut-off frequency of the shell structure.

The effects of the piezoelectric layer are studied by changing the thickness of the layer. Since the stiffness of PZT-4 is smaller than that of aluminium and steel, but greater than that of gold, the results show that with the increase of the piezoelectric layer, the phase velocities and the cut-off frequency decrease for the aluminium and steel as core materials in the shell. The inverse trend is found for the shell with gold as core materials. The results of phase velocities and cut-off frequency in the limit cases for large and small wavelength are also obtained by theoretical deduction.

The results of this paper can serve as a reference for future study on wave propagation in piezoelectric coupled structures as well as in the design of smart structures incorporating piezoelectric materials. The further work will focus on the wave propagation in the piezoelectric coupled cylindrical shells by more general shell theories to account for the effects of shear and bending to improve the results.

Acknowledgements

The work in this paper is supported by the research grant from National University of Singapore, R-264-000-113-112.

References

Bailey, T., Hubbard Jr., J.E, 1985. Distributed piezoelectric polymer active vibration control of a cantilever beam. J. Guidance Contr. Dyn. 8, 605–611.

Bleustein, J.L., 1969. Some simple modes of wave propagation in an infinite piezoelectric plates. J. Acoust. Soc. Am. 45, 614–620.

Crawley, E.F., de Luis, J., 1987. Use of piezoelectric actuators as elements of intelligent structures. AIAA J. 25, 1373–1385.

Cooper, R.M., Naghdi, P.M., 1957. Propagation of nonaxially symmetric waves in elastic cylindrical shells. J. Acoust. Soc. Am. 29, 1365–1372.

Curtis, R.G., Redwood, M., 1973. Transverse surface waves in piezoelectric materials carrying a metal layer of finite thickness. J. Appl. Phys. 44, 2002–2007.

Donnel, L.H., 1933. Stability of thin walled tubes under torsion. NACA Rep. No. 479.

Flügger, W., 1934. Satik und Dynamik der Schalen. Springer, Berlin.

Graff, K.F., 1991. Wave Motion in Elastic Solids. Dover Publications, New York.

Lin, T.C., Morgan, G.W., 1956. A study of axisymmetric vibrations of cylindrical shells as affected by rotatory inertia and transverse shear. J. Appl. Mech. 23, 255–261.

Love, A.E.H., 1944. A Treatise on the Mathematical Theory of Elasticity. Dover Publication, New York.

Mirsky, I., Herrmann, G., 1958. Axially symmetric motions of thick cylindrical shells. J. Appl. Mech. 25, 97–102.

Mindlin, R.D., 1952. Forced thickness-shear and flexural vibrations of piezoelectric crystal plates. J. Appl. Phys. 23, 83–88.

Quek, S.T., Wang, Q., 2001. On dispersion relations in piezoelectric coupled plate structures. Smart Mater. Struct. 9, 859–867.

Sanders, J.L., 1959. An improved first approximation theory for thin shells. NASA Tech. Rep. R24.

Sun, C.T., Cheng, N.C., 1974. Piezoelectric waves on a layered cylinder. J. Appl. Phys. 45, 4288–4294.

Tiersten, H.F., 1963. Wave propagation in an infinite piezoelectric plate. J. Acoust. Soc. Am. 35, 234–239.

Varadan, V.V., Jeng, J.H., Varadan, V.K., 1987. Form invariant constitutive relations for transversely isotropic piezoelectric materials. J. Acoust. Soc. Am. 82, 337–341.

Viktorov, I.A., 1967. Rayleigh and Lamb Waves. Plenum, New York.

Viktorov, I.A., 1981. Surface Waves in Solids. Nauka, Moscow, in Russian.

Vlasov, V.Z., 1949. General Theory of Shells and its Application to Engineering. Leninggrad, Moscow.

Wang, B.T., Rogers, C.A., 1991. Laminate plate theory for spatially distributed induced strain actuators. J. Comp. Mater. 25, 433–452.

Wang, Q., Quek, S.T., 2001. On dispersion relations in piezoelectric coupled beams. AIAA J. 38, 2357–2361.